A New Vibrational Control System in Nature: Flapping Flight

Haithem Taha* and Mohammadali Kiani†

University of California, Irvine, CA 92697

Vibrational control is an open loop stabilization technique via the application of high-amplitude, high-frequency oscillatory inputs. The averaging theory has been the standard technique for designing vibrational control systems. However, it stipulates too high oscillation frequency that may not be practically feasible. Therefore, although vibrational control is very robust and elegant (stabilization without feedback), it is rarely used in practical applications. The only well-known example is the Kapitza pendulum; an inverted pendulum shose pivot is subject to vertical oscillation. the unstable equilibrium of the inverted pendulum gains asymptotic stability due to the high-frequency oscillation of the pivot. In this paper, we provide a new vibrational control system from Nature; flapping flight dynamics. Flapping flight is a rich dynamical system as a representative model will typically be nonlinear, time-varying, multi-body, multi-time-scale dynamical system. Over the last two decades, using direct averaging, there has been consensus in the flapping flight dynamics community that insects are unstable at the hovering equilibrium due to the lack of pitch stiffness. In this work, we perform higher-order averaging of the time-periodic dynamics of flapping flight to show a vibrational control mechanism due to the oscillation of the driving aerodynamic forces. We also experimentally demonstrate such a phenomenon on a flapping apparatus that has two degrees of freedom: forward translation and pitching motion. It is found that the time-periodic dynamics of the flapping micro-air-vehicle is naturally (without feedback) stabilized beyond a certain threshold. Moreover, if the averaged aerodynamic thrust force is produced by a propeller revolving at a constant speed while maintaining the wings stationary at their mean positions, no stabilization is observed. Hence, it is concluded that the observed stabilization in the flapping system at high frequencies is due to the oscillation of the driving aerodynamic force and, as such, flapping flight indeed enjoys vibrational stabilization.

I. Introduction

Vibrational control is an open loop stabilization technique of an unstable equilibrium via the application of a sufficiently high-amplitude, high-frequency periodic forcing. It was first introduced under this name by Meerkov[1] for linear time-varying systems. A typical example that demonstrates such a phenomenon is the Stephenson-Kapitza pendulum: an inverted pendulum whose pivot is subject to a vertical oscillation. The unstable equilibrium of the inverted pendulum gains asymptotic stability when the pivot is oscillating vertically at a sufficiently high frequency. This phenomenon is referred to as vibrational stabilization/control and has been first introduced by Stephenson[2] who analyzed it using a periodic series solution and later by Kapitza[3,4] using an averaged potential approach.

By definition, vibrationally-controlled systems are typically time-periodic systems. The standard and most convenient technique of analyzing nonlinear time-periodic (NLTP) systems is averaging.[5] In this approach, one averages the NLTP system over the fast time scale to obtain a nonlinear, time-invariant (NLTI) system. As such, if an equilibrium state of the NLTP system is represented by a periodic orbit, it reduces to a fixed point of the NLTI system. Clearly, analyzing the stability of a fixed point of a time-invariant system is much easier than analyzing the stability of a periodic orbit of a time-varying system. Then, for *high enough* oscillation frequency, the averaging theorem guarantees that exponential stability of a

*Assistant Professor, Mechanical and Aerospace Engineering, AIAA Member.

†Master Student, Mechanical and Aerospace Engineering, AIAA Member.

fixed point for the NLTI model implies exponential stability of the corresponding periodic orbit of the NLTP system.[6] To determine exponential stability of the fixed point, one may simply linearize the NLTI system to obtain a linear, time-invariant (LTI) model and examine the eigenvalues of the state matrix for the LTI system.

Although vibrational stabilization is well-known for its robustness[7] and elegancy (stabilization without feedback), it has been rarely exploited in practical applications because of the very high-frequency requirement that is typically dictated by the averaging theory as pointed out by Berg and Wickramasinghe.[8] Probably, the Kapitza pendulum (inverted pendulum subject to vertical oscillation) is the only widely known example. In this paper, we provide a new vibrational control system that is designed by Nature. We show that flapping flight enjoys a natural stabilization due to the periodic nature of the driving aerodynamic forces.

Biological flyers represent a gold mine of scientifically-rich problems and a well-spring of knowledge and inspiration for engineers and scientists. For example, some insects can thrust up to five times their weights,[9] while others have been observed to perform turning maneuvers of greater than 3000 deg/s, with less than a 30 ms delay,[10] in situations that demand agility, such as chasing a potential mate. In normal everyday flight, birds may experience up to 14 g accelerations in super-maneuverable tasks,[11] while the maneuverability of the most advanced fighter airplanes cannot exceed $8-9$ g. Moreover, birds and insects outperform jet airplanes more than five times from a normalized power consumption perspective.[11] This huge potential inspired engineers to design flapping micro-air-vehicles (MAVs),[12] mainly for reconnaissance and surveillance applications.

Indeed, flapping flight invokes and pushes the frontiers of mechanical and aerospace engineering disciplines. From an aerodynamic point of view, flapping flight creates an unsteady, nonlinear flow field exploiting unconventional mechanisms to generate lift. In fact, using classical aerodynamics, insect flight was deemed impossible for decades (e.g.,[13–16]), as the required lift coefficients for balance are $2-3$ times the maximum lift coefficients achieved by conventional aerodynamics. Then, biologists and engineers unraveled some of the unconventional lift mechanisms exploited by insect and bird flight. A stabilized leading edge vortex, first introduced by Ellington and his coworkers,[17] forms the main unconventional lift mechanism that makes insect flight possible. Computational fluid dynamic simulations show that the leading edge vortex contributes 40% of the total lift for insects.[18]

As the aerodynamics of flapping flight became mature, the flight dynamic analysis followed promptly; to our knowledge, the first article on flapping flight dynamics is that of Thomas and Taylor.[19] Flapping flight dynamics represents a multi-body, nonlinear time-periodic (NLTP) dynamical system. Moreover, it is a multi-scale dynamical system because of the concomitant two time scales: the fast time scale of the flapping motion and the associated aerodynamic loads, and the relatively slow time scale of the body motion. All these challenges make flapping flight dynamics an intricate problem that necessitates a rigorous mathematical analysis.

Direct averaging has been the standard technique of analyzing the NLTP dynamics of flapping flight,[10, 20–30] relying on the large separation between the system's two time scales; the ratio of the forcing flapping frequency to the natural frequency of the body motion is about 30 for one of the slowest flapping insects (the hawkmoth). Using direct averaging, there has been a consensus among the flapping flight dynamics community that insects are unstable at the hovering equilibrium. This instability is mainly attributed to lack of pitch stiffness, which is instrumental to static and dynamic stability of conventional airplanes where pitch stiffness is mainly ensured by the horizontal tail.[31] Insects do not possess horizontal tails. Moreover, even the existence of horizontal tails would not avail in the hovering position at zero forward speed.

Note that crude averaging of the simple equations governing the dynamics of the Kapitza pendulum[3, 4] showed no stabilization due to the pivot vibration. However, appropriate averaging techniques, whether it is higher-order averaging[32, 33] based on chronological calculus,[34] higher-order averaging[35, 36] based on Lie transform,[37] direct averaging exploiting the nonlinear variation of constants formula,[38, 39] clearly show a vibrationally-induced stabilizing stiffness.

In this work, we performed second-order averaging[5, 32, 33] based on chronological calculus[34] to analyze the NLTP dynamics of flapping flight and show a vibrationally-induced pitch stiffness mechanism. The analytical nature of the developed flight dynamic model and the adopted analysis tool allowed scrutiny of the system dynamics that revealed the physics of this unconventional stabilization. It is found that the interaction between the forward (or normal) body motion with the wing back-and-forth oscillatory motion is the main source of such an unconventional stiffness mechanism. Therefore, we experimentally demonstrated such a phenomenon on a flapping apparatus that allows two degrees-of-freedom (DOF) for the body of a flapping MAV: forward motion and pitching motion.

II. Flight Dynamics of Flapping MAVs

A. Flight Dynamic Modeling

Figure 1 shows a schematic diagram for a flapping animal (or a MAV) in the longitudinal plane $x - z$ with three DOFs: translations along the x and z axes with velocity components u and w, respectively, and a rotation about the y axis (into the page) represented by an angle θ and an angular velocity q. The generalized forces X and Z are the aerodynamic forces in the x- and z-directions, respectively, and M is the aerodynamic pitching moment about the y-axis.

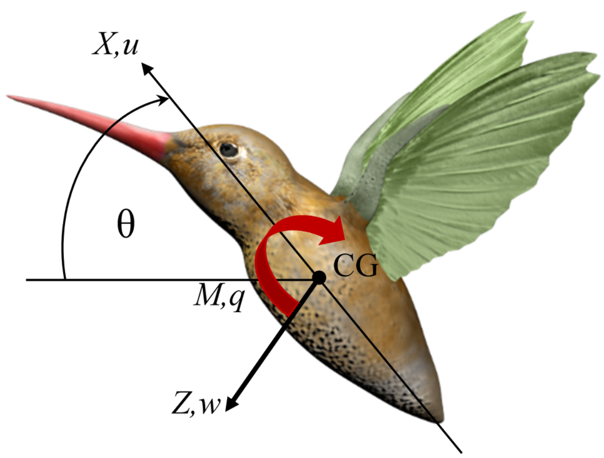

Figure 1. Schematic diagram of a flapping animal in the longitudinal plane $x - z$.

Ignoring the wing structural and inertial effects, the longitudinal equations of motion are exactly the same as conventional aircraft[31]

$$\begin{pmatrix} \dot{u} \\ \dot{w} \\ \dot{q} \\ \dot{\theta} \end{pmatrix} = \begin{pmatrix} -qw - g\sin\theta \\ qu + g\cos\theta \\ 0 \\ q \end{pmatrix} + \begin{pmatrix} X/m \\ Z/m \\ M/I_y \\ 0 \end{pmatrix}, \quad (1)$$

where g is the gravitational acceleration, m is the body mass, and I_y is the body pitching inertia. However, unlike conventional aircraft, the aerodynamic loads X, Z, and M are essentially time-varying. That is, the system (1) can be written in the abstract form

$$\dot{\boldsymbol{x}}(t) = \boldsymbol{F}(\boldsymbol{x}(t), \tau) = \boldsymbol{f}(\boldsymbol{x}(t)) + \boldsymbol{g}_a(\boldsymbol{x}(t), \tau), \quad (2)$$

where the aerodynamic vector field $\boldsymbol{g}_a$ is time varying.

It is quite important to note that two symbols t and τ are used in Eq. (2) to denote the independent time variable: to distinguish between the slow time scale t associated with the body motion and the fast time scale of the flapping motion and the concomitant aerodynamic loads. The ratio between these two time scales is deceptively large; for one of the slowest flapping insect (the hawkmoth), the ratio between the flapping frequency and the flight dynamics natural frequency is around 30,[23,40,41] which naturally invokes averaging. That is, the aerodynamic loads oscillate with a too high frequency to affect the body. In other words, the body only responds to the mean values of the time-periodic aerodynamic loads. This assumption is found in most of flapping flight dynamics and control efforts.[?,10,19–24,26–28,42–48] Adopting this averaging assumption, the averaged dynamics of the system (2) is written as

$$\dot{\bar{\boldsymbol{x}}} = \bar{\boldsymbol{F}}(\boldsymbol{x}(t)) = \boldsymbol{f}(\bar{\boldsymbol{x}}) + \bar{\boldsymbol{g}}_a(\bar{\boldsymbol{x}}), \quad (3)$$

where over bar indicates an averaged quantity; e.g., $\bar{\boldsymbol{g}}_a(\boldsymbol{x}) = \frac{1}{T}\int_0^T \boldsymbol{g}_a(\boldsymbol{x}, \tau)d\tau$, with T being the flapping period.

Following our previously derived aerodynamic model,[40,49] which is based on Refs.,[50–52] the aerodynamic loads can be expressed linearly in the state variables $\boldsymbol{x}$, near the hovering position as

$$\boldsymbol{g}_a(\boldsymbol{x}(t), \tau) = \boldsymbol{g}_0(\tau) + [\boldsymbol{G}(\tau)]\,\boldsymbol{x}(t), \quad (4)$$

where $\boldsymbol{g}_0$ represents the aerodynamic loads due to flapping, ignoring the effect of body motion (i.e., ignoring aerodynamic-dynamic interactions), and the matrix $\boldsymbol{G}$ represents the aerodynamic derivatives (i.e., stability derivatives) with respect to the state variables. Expressions of the various terms in $\boldsymbol{g}_0$ and $\boldsymbol{G}$ are given in terms of the flapping kinematics in our previous efforts[5,40,49] as

$$\boldsymbol{g}_0(t) = \begin{pmatrix} X_0(t)/m \\ Z_0(t)/m \\ M_0(t)/I_y \\ 0 \end{pmatrix} \quad \text{and} \quad \boldsymbol{G}(t) = \begin{bmatrix} X_u(t) & X_w(t) & X_q(t) & 0 \\ Z_u(t) & Z_w(t) & Z_q(t) & 0 \\ M_u(t) & M_w(t) & M_q(t) & 0 \\ 0 & 0 & 0 & 0 \end{bmatrix},$$

where the different entries are defined below.

Assuming a horizontal stroke plane, parameterized by the "back-and-forth" flapping angle φ, and a piecewise constant variation in the wing pitch angle η, one obtains[40]

$$X_0(t) = -2K_{21}\dot{\varphi}(t)|\dot{\varphi}(t)|\cos\varphi(t)\sin^2\eta \;\;,\;\; Z_0(t) = -K_{21}\dot{\varphi}(t)|\dot{\varphi}(t)|\sin 2\eta$$

$$M_0(t) \;\;=\;\; 2\dot{\varphi}(t)|\dot{\varphi}(t)|\sin\eta[K_{22}\Delta\hat{x}\cos\varphi(t) + K_{21}x_h\cos\eta(t) + K_{31}\sin\varphi(t)\cos\eta]$$

where x_h is the distance from the vehicle center of mass to the root of the wing hinge line (i.e., the intersection of the hinge line with the x-axis) and $\Delta\hat{x}$ is the chordwise distance from the center of pressure to this same hinge location, normalized by the chord length. Also, ρ is the air density, C_{L_α} is the three-dimensional lift curve slope of the wing, $c(r)$ is the spanwise chord distribution, R is the wing radius, $I_{mn} = 2\int_0^R r^m c^n(r)\,dr$, and $K_{mn} = \frac{1}{4}\rho C_{L_\alpha} I_{mn}$. The time-varying stability derivatives are written directly in terms of the system parameters as[40]

$$X_u = -4\tfrac{K_{11}}{m}|\dot{\varphi}|\cos^2\varphi\sin^2\eta, \quad X_w = -\tfrac{K_{11}}{m}|\dot{\varphi}|\cos\varphi\sin 2\eta, \quad X_q = \tfrac{K_{21}}{m}|\dot{\varphi}|\sin\varphi\cos\varphi\sin 2\eta - x_h X_w$$

$$Z_u = 2X_w, \quad Z_w = -2\tfrac{K_{11}}{m}|\dot{\varphi}|\cos^2\eta, \quad Z_q = 2\tfrac{K_{21}}{m}|\dot{\varphi}|\sin\varphi\cos^2\eta - \tfrac{K_{rot_{12}}}{m}\dot{\varphi}\cos\varphi - x_h Z_w$$

$$M_u = 4\frac{K_{12}\Delta\hat{x}}{I_y}|\dot{\varphi}|\cos^2\varphi\sin\eta + \frac{m}{I_y}\left(2X_q - x_h Z_u\right)$$

$$M_w = 2\frac{K_{12}\Delta\hat{x}}{I_y}|\dot{\varphi}|\cos\varphi\cos\eta + 2\frac{K_{21}}{I_y}|\dot{\varphi}|\sin\varphi\cos^2\eta - \frac{m x_h}{I_y}Zw$$

$$\begin{aligned} M_q \;\;=\;\; & -\tfrac{2\Delta\hat{x}}{I_y}|\dot{\varphi}|\cos\varphi\cos\eta\left(K_{12}x_h + K_{22}\sin\varphi\right) + \tfrac{1}{I_y}\dot{\varphi}\cos\varphi\left(K_{rot_{13}}\Delta\hat{x}\cos\varphi\cos\eta + K_{rot_{22}}\sin\varphi\right) + \\ - \;\; & \tfrac{2}{I_y}|\dot{\varphi}|\cos^2\eta\sin\varphi\left(K_{21}x_h + K_{31}\sin\varphi\right) - \tfrac{K_v\mu_1 f}{I_y}\cos^2\varphi - \tfrac{m x_h}{I_y}Z_q \end{aligned}$$

where $K_{rot_{mn}} = \pi\rho(\frac{1}{2} - \Delta\hat{x})I_{mn}$ and $K_v = \frac{\pi}{16}\rho I_{04}$. The hinge line is set at $30\%c$ ($\Delta\hat{x} = 0.05$), x_h is assumed zero for simplicity, and the value of C_{L_α} is calculated based on the wing aspect ratio using the extended lifting theory according to Taha et al.[51] The above flight dynamic model has been developed in Ref.[40] and the resulting eigenvalues of the averaged, linearized dynamics have been validated against numerical simulations of Navier-Stokes equations by Sun et al.[23] and the experimental data of Cheng and Deng.[30]

B. Stability Analysis Using Direct Averaging

Direct averaging greatly simplifies the problem as it converts the time-periodic system (2) into a time-invariant system (3). Consequently, a periodic orbit representing an equilibrium solution of (2) reduces to a fixed point of the averaged dynamics (3). Clearly, the stability analysis of a fixed point of a time-invariant system is quite simpler than that of a periodic solution for a time-periodic system. Luckily, the averaging theorem[6,38] guarantees exponential stability of a periodic solution of (2) if the corresponding fixed point of (3) is exponentially stable.

To focus on the open-loop stability, we will exclude the non-trivial balance problem in this paper; that is, we assume that the flapping MAV is balanced at hover; i.e., equivalently, the averaged dynamics has a fixed point at the origin

$$\boldsymbol{f}(\boldsymbol{0}) + \bar{\boldsymbol{g}}_0 = \boldsymbol{0} \Longleftrightarrow \bar{Z}_0 = -mg.$$

Then, linearizing the averaged dynamics (3) about this fixed point at the origin yields

$$\dot{\bar{\boldsymbol{x}}}(t) = \left[D\boldsymbol{f}(\boldsymbol{0}) + \bar{\boldsymbol{G}}\right]\bar{\boldsymbol{x}}(t), \tag{5}$$

where $D\boldsymbol{f}(\mathbf{0})$ is the jacobian of the vector field $\boldsymbol{f}$ at the origin and $\bar{\boldsymbol{G}}$ represents the cycle-averaged stability derivatives. Evaluating the matrix of the linearized system (5) for the hawkmoth insect, whose morphological parameters are adopted from Refs.,[5,23,53] one obtains

$$\left[D\boldsymbol{f}(\mathbf{0})+\bar{\boldsymbol{G}}\right]=\begin{bmatrix} -3.59 & 0 & 0 & -9.81 \\ 0 & -3.30 & 0 & 0 \\ 39.95 & 0 & -7.92 & 0 \\ 0 & 0 & 1 & 0 \end{bmatrix}$$

whose eigenvalues are written as

$$0.19 \pm 5.74i,\ -11.89,\ -3.30.$$

These eigenvalues indicate an unstable system due to the pair in the right half plane, which are mainly associated with pitching motion as can be easily shown by checking the corresponding eigenvectors. This result is well known and has been concluded in several efforts.[20,22–24,29,30,40,42,54–56]

III. Higher-Order Averaging and Vibrational Control

As in the case with the Kapitza pendulum, the crude averaging analysis, explained above, does not capture vibrational stabilization. One remedy is to use the variation of constants formula (coordinate transformation) to write the system (2) in the standard form of first-order averaging. However, this process is not analytically tractable here. Alternatively, one can use higher-order averaging to reveal higher-order interactions between the system's two time scales that are typically neglected by direct averaging.

Agrachev and Gamkrelidze wrote a seminal paper[34] in the honor of the 70^{th} birth day of the pioneer Russian mathematician Lev Semyonovich Pontryagin which laid down the foundation of a new calculus for time-varying vector fields: the *chronological calculus*. Based on these tools, Sarychev[32] and Vela[33] developed what they called the *complete averaging* of the time-periodic system (2) as an infinite series

$$\dot{\overline{\boldsymbol{x}}} = \epsilon\boldsymbol{\Lambda}_1(\overline{\boldsymbol{x}}) + \epsilon^2\boldsymbol{\Lambda}_2(\overline{\boldsymbol{x}}) + ..., \tag{6}$$

where ϵ is a small parameter, typically scaled with the reciprocal of the forcing frequency, and

$$\begin{aligned} \boldsymbol{\Lambda}_1(\overline{\boldsymbol{x}}) &= \tfrac{1}{T}\int_0^T \boldsymbol{F}(\boldsymbol{x},\tau)\,d\tau, \\ \boldsymbol{\Lambda}_2(\overline{\boldsymbol{x}}) &= \tfrac{1}{2T}\int_0^T \left[\int_0^\tau \boldsymbol{F}(\boldsymbol{x},s)\,ds, \boldsymbol{F}(\boldsymbol{x},\tau)\right]\,d\tau. \end{aligned}$$

So, if the flapping frequency is high enough (i.e., ϵ is small enough), one may be able to truncate the series (6) after the first term $\boldsymbol{\Lambda}_1$ (i.e., crude averaging). However, if the flapping frequency is not high, one should take into account more terms in the series. For more details about this approach, the reader is referred to the Refs.[5,32,33]

Taking two terms in the series (6) and linearizing about the origin, one obtains the following system matrix for the hawkmoth linearized hovering dynamics

$$D(\boldsymbol{\Lambda}_1+\boldsymbol{\Lambda}_2)(\mathbf{0})=\begin{bmatrix} -3.58 & 0 & 0 & -9.81 \\ 0 & -3.09 & 0 & 0 \\ 29.98 & 0 & -8.13 & -28.45 \\ -2.90 & 0 & 0.96 & 0 \end{bmatrix}$$

whose eigenvalues are written as

$$-0.66 \pm 3.72i,\ -10.40,\ -3.09$$

which indicate a stable system.

This stabilization is not captured by crude averaging. To determine the nature of this *vibrarional stabilizing* mechanism, which is induced by higher-order interactions between the system's two times scales, we compare the two matrices $D(\boldsymbol{\Lambda}_1)(\mathbf{0})$, $D(\boldsymbol{\Lambda}_1+\boldsymbol{\Lambda}_2)(\mathbf{0})$ of the first- and second-order averaged dynamics, respectively. Of particular interest is the element (3,4), which represents pitch stiffness. It is found that the original hovering flight dynamics of insects and flapping MAVs lacks any *direct* pitch-stiffness.[40] However, higher-order averaging revealed a vibrationally-induced pitch-stiffness, which is written as

$$\dot{\bar{q}} = \ddot{\bar{\theta}} = -28.45\bar{\theta}.$$

This vibrational control stiffness is quite similar to the Kapitza pendulum case.

Thanks to the analytical nature of the presented model and analysis tool, we managed to drive an analytical expression of this vibrationally induced stiffness as

$$k_\theta = \frac{g}{2T}\int_0^T \left[\left(M_u(t)t - \int_0^t M_u(\tau)d\tau\right)\cos\theta_e + \left(M_w(t)t - \int_0^t M_w(\tau)d\tau\right)\sin\theta_e\right]dt, \tag{7}$$

where M_u and M_w are the resulting pitching moments due to disturbances in the body forward and normal speeds, respectively, and θ_e is the inclination angle of the body longitudinal x axis on the horizontal plane at hovering. For zero θ_e and x_h (as in the analysis above), the first-order contribution of k_θ can be written in terms of the insect morphological parameters as

$$k_\theta = \frac{mg^2 f(\Phi)}{2I_y \bar{\dot{\varphi}}^2}, \tag{8}$$

where Φ is the flapping amplitude, $\bar{\dot{\varphi}}$ is the average flapping speed, and $f(\Phi) = \frac{\sin 2\Phi}{2\Phi} - \cos 2\Phi$. Equation (7) implies that the vibrationally-induced stiffness k_θ is due to the variation of the stability derivatives M_u and/or M_w over the cycle: if M_u and M_w are constants (or replaced with their averaged values), k_θ will be zero. Note that the oscillation of M_u and M_w over the flapping cycle is mainly due to the wing oscillatory motion. That is, physically, k_θ is due to interaction between the body forward or normal translatory motion and the wing oscillatory motion.

IV. Experimental Setup

A. One Degree of Freedom Flapping MAV

From the above discussion, demonstration of vibrational stabilization in flapping flight requires at least two degrees of of freedom (DOFs) for the body: transaltory motion and pitching motion. Therefore, in order to avoid the many problems associated with free flight and to have a better focus on verifying the vibrational stabilization phenomenon, we construct an experimental setup that allows for these two degrees of freedom only. Imagine a simple pendulum with its mass replaced by a MAV, as shown in the schematic in Fig. 2(a). The hovering equilibrium is then achieved when the pendulum's rod becomes horizontal, as shown in the real picture of our realization presented in Fig. 2(b). This system represents the simplest configuration with a single DOF (the pendulum angle γ) that mimics the transaltory motion of the body.

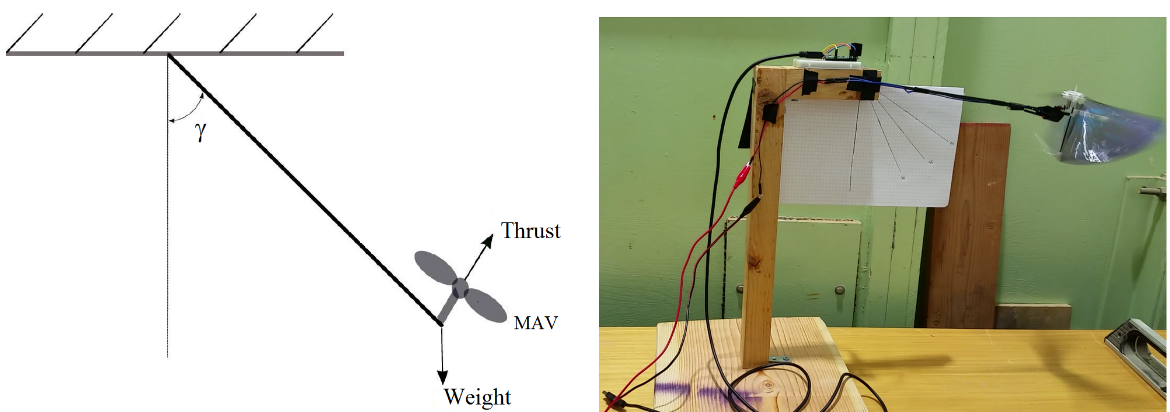

(a) A Pendulum-MAV Schematic. (b) Realization of the Schematic.

Figure 2. The experimental setup of a pendulum-like flapping MAV.

This pendulum-like setup is preferred in comparison to the Wood's Harvard Robofly[12] (moving along vertical rails), which was used to prove the concept of flapping MAVs. Note that for the latter configuration, if the flapping amplitude/frequency is slightly deviated from the hovering balance requirement, the MAV will experience a vertical climb/descent with some mean velocity. In contrast, because of the gravitational spring action provided by the pendulum configuration, any deviation from the hovering balance requirement results in a slightly different equilibrium *position* γ_e. In addition, measurement of this equilibrium pendulum angle γ_e is easily achieved using a Gravity 360 Degree Hall Angle Sensor[57] and provides a measure for the generated thrust from the flapping MAV as the flapping frequency changes, according to the balance equation

$$F_T = \left(m_{\text{MAV}} + \frac{1}{2} m_{\text{rod}} \right) g \sin \gamma_e,$$

where F_T is the cycle-averaged generated thrust force, m_{MAV} is the mass of the flapping MAV (13 gm), m_{rod} is the mass of the pendulum's rod (1.8 gm), and g is the gravitational acceleration. The power supply in the lab already provides information about the cycle-averaged total power consumption P. As the applied voltage is increased, the flapping frequency increases. Sp, at each given voltage, a video is recorded at a rate of 240 frame per second; the time stamp of each video is analyzed to obtain an estimate for the flapping frequency (the average flaps per second). As such, the performance characteristics of the flapping MAV is determined and presented in Fig. 3.

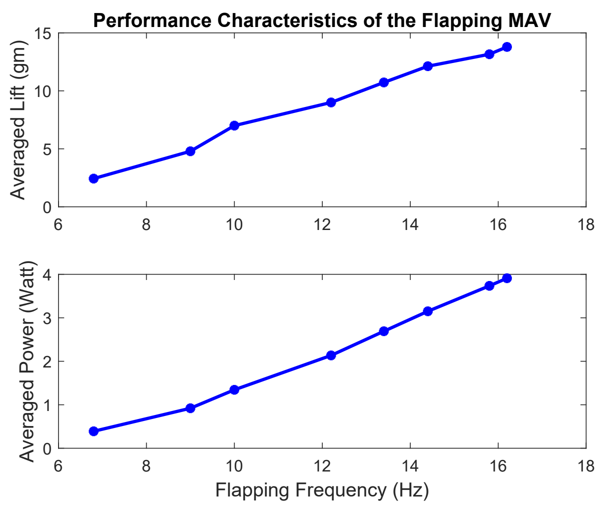

Figure 3. Performance characteristics of the used flapping MAV.

The adopted flapping MAV is an off-the-shelf flapping bird[58] whose wings are highly flexible wings that flap in a vertical stroke plane resulting in a good thrust producing capability at zero forward speed (i.e., at the hovering position). This flapping MAV (shown in Fig. 4(a)) is adapted for the current experimental setup as shown in Fig. 4(b); only the wings and the flapping mechanism are retained while the body and motor are replaced. Of particular importance is the replacement of the driving motor with a stronger motor[59] that allows operating at higher flapping frequencies, which is necessary for the demonstration of vibrational stabilization.

B. Two Degrees of Freedom Flapping MAV

A pin (hinge) connection is introduced between the body of the MAV and the pendulum's rod to allow for body pitching θ, as shown in Fig. 5(a). The response of the pitching angle is measured using a digital camera and an image processing algorithm (e.g.,[60]). As shown in Figs. 4(b), 5(a), the nose and tail of the MAV are marked with different colors. Then, a simple algorithm is implemented in Visual Studio C++, exploiting the image processing library OpenCV, to detect these circular stickers from video recordings and determine the angle between the line connecting these two marks and the horizontal (i.e. θ) at each time stamp with a sampling frequency of 50 ms.

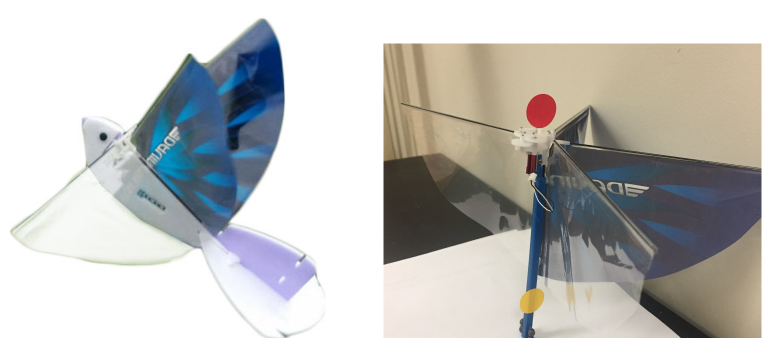

(a) Actual Bird.[58] (b) Adapted Version of the MAV.

Figure 4. The actual and adapted flapping MAVs.

Because the line of action of the thrust force is above the body longitudinal axis and consequently hinge point, there is an unbalanced pitching moment which will preclude equilibria. Therefore, we added four split shot size lead of 3g total weight near the tail of the flapping MAV, as shown in Figs. 4(b),5(a) (the black dots near tail) to shift the center of gravity of the MAV backward along the longitudinal axis. As such, the pitching moment at the hinge point due to the weight will balance that of the thrust force according to the balance equation

$$F_T e_T = m_{\mathrm{MAV}} g e_g \cos\theta_e,$$

where e_T and e_g are the offsets of the thrust and gravity forces, respectively, from the hinge point, and θ_e is the equilibrium value of the pitching angle. At zero applied voltage (zero thrust force), the flapping MAV is standing vertically ($\theta_e = 90°$) at the bottom position ($\gamma_e = 0°$) of the pendulum. As the voltage and consequently the flapping frequency increase, the body moves upward along the circular path of the pendulum (i.e., γ increases) and tilts forward towards the horizontal attitude (i.e., θ decreases), as shown in Fig. 5(a). It is noteworthy that most insects have their center of gravity behind the hinge location along their longitudinal axis and achieve hovering equilibria at body inclination with respect to the horizontal (i.e., θ_e) around 50°,[23,53] similar to the current setup.

V. Experimental Demonstration of Vibrational Stabilization in Flapping Flight

Having established equilibrium, studying stability comes promptly. It is noteworthy that most research reports concluded instability of insects and flapping MAVs at hover due to lack of pitch stiffness.[22,23,25,29,30,40,56,61,62] Hence, it has been believed that insects and their man-made flapping MAVs have to employ feedback to stabilize their flight during hover. While this may indeed be true, these studies mostly neglected the potential of the natural high-frequency oscillatory flapping motion to induce vibrational stabilization.[5,63] To experimentally verify and demonstrate such a phenomenon in flapping MAVs, we apply different voltages to the motor driving the flapping mechanism to attain different equilibrium positions (γ_e and θ_e) at different flapping frequencies, thanks to the pendulum configuration and to the stronger motor. We then measure the response of the pendulum angle γ and the body pitching angle θ, as explained above, at each operating frequency.

Figure 5(b) shows the response of the flapping MAV system at a flapping frequency of $\sim$ 12Hz (corresponding to 1.94 Volt). At this low flapping frequency, the MAV barely goes up ($\gamma_e \sim 24°$) and the equilibrium pitching angle is quite large ($\theta_e \sim 76°$). The response is found to be unstable as shown in the figure, even without giving a disturbance: the oscillatory wing motion naturally provides a sufficient disturbance.

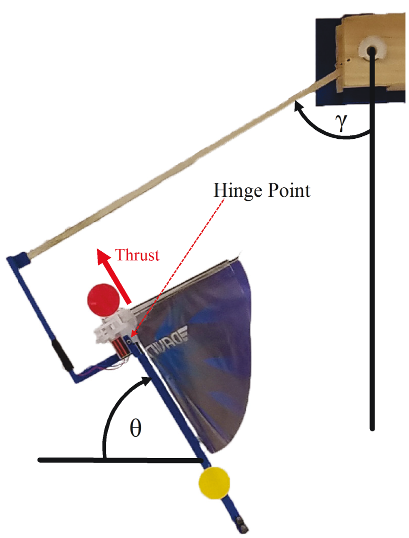

(a) Two-DOF Flapping MAV Experimental Setup.

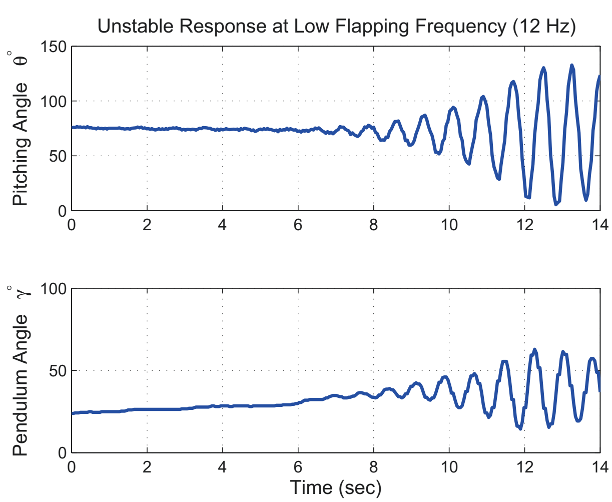

(b) MAV unstable response at relatively low flapping frequency ($\sim$ 12Hz).

Figure 5. A two-DOF MAV setup and its unstable response at low flapping frequency.

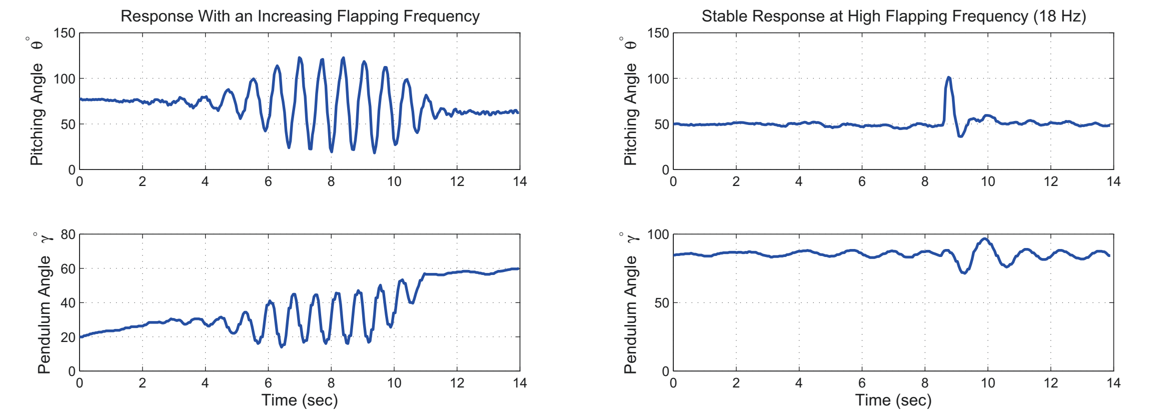

(a) MAV response as the flapping frequency is being manually increased.

(b) MAV stable response at relatively high flapping frequency ($\sim$ 18Hz).

Figure 6. MAV response is stabilized as the flapping frequency is increased.

Figure 6(a) shows the response of the flapping MAV system as the applied voltage (flapping frequency) is manually increased from 1V to 3V. The bird rises up towards the hovering position (γ goes from 20° to 60° and θ changes from 77° to 62°). It is clear that the flapping MAV response experiences instability during the transition period and becomes stable beyond a certain pendulum angle (i.e., flapping frequency). We apply fixed different voltages (corresponding to different flapping frequencies) and observe the system response at each case. The threshold flapping frequency below which the MAV response is unstable and beyond which it is naturally stabilized is found to be 15Hz. It is envisaged that this threshold should be related to the system's natural frequency (1.4Hz). That is, the stabilization-threshold ratio between the periodic forcing frequency and the system's natural frequency is found to be 10.7 for the current setup. Seeking a universal value for such a ratio is quite important and is suggested for future work.

Figure 6(b) shows the response of the flapping MAV system at a relatively high flapping frequency of $\sim$ 18Hz (corresponding to 3 Volt). At this relatively high flapping frequency, the MAV system is almost at the hovering position ($\gamma_e \sim 85°$) and the equilibrium pitching angle $\theta_e \sim 50°$ is close to the natural values observed in nature for hovering insects.[23,53] Clearly, the response is stable. Even when a relatively large disturbance ($\Delta\theta \sim 50°$) is applied at $t = 8.6$ sec, the system goes back to its equilibrium periodic orbit (i.e., the hovering periodic orbit).

So far, it can be concluded that the response of flapping MAVs (particularly the body pitch response) is naturally (without feedback) stabilized beyond a certain threshold of flapping frequency. This fact conforms well with the vibrational stabilization phenomenon[2–4,8] and suggests that the observed natural stabilization at high frequencies is a vibrational stabilization phenomenon. However, one might argue that because the intricate dynamics of the system, the frequency not only affects stability, but also balance/equilibrium; obviously increasing the frequency leads to a different equilibrium, which may or may not have similar stability characteristics to equilibria corresponding to low frequencies. To show that the induced stabilizing mechanism is indeed a vibrational stabilization one that is mainly due to the time-periodic nature of the driving aerodynamic thrust force and not because of operating at a different equilibrium, we construct a replica of the experimental setup with the MAV wings being fixed at their mean position and a small propeller revolving with a constant speed is added, as shown in Fig. 7(a). The main difference is that the flapping MAV setup produces a periodic thrust force, and consequently a time-periodic dynamics allowing for vibrational stabilization, while the propeller setup produces a constant thrust force, and consequently a time-invariant dynamics leaving no room for vibrational stabilization.

Using split shot size lead, we managed to match the weight and inertia of the propeller system with the flapping MAV system. Moreover, since the propeller is providing a constant thrust force equal to the averaged thrust from the flapping wings, the propeller system can be thought of as the averaged dynamics of the flapping MAV system. Figure 7(b) shows the response of the two-DOF propeller-pendulum system at a relatively small propeller speed (i.e., at a small pendulum equilibrium angle $\gamma_e \sim 9°$). Clearly, the response is exponentially unstable. Increasing the applied voltage to attain higher pendulum equilibrium angles (closer to the hovering position) worsens the stability characteristics so much that the system structure becomes

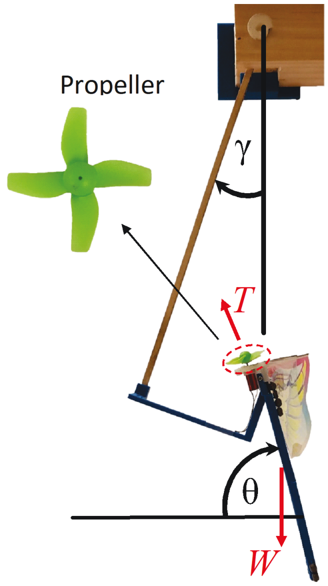

(a) A Two-DOF MAV-Propeller Setup.

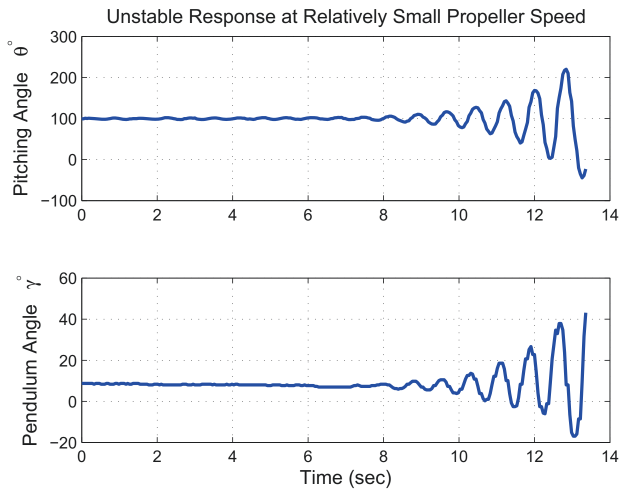

(b) Unstable Response of the Two-DOF MAV-Propeller System.

Figure 7. A two-DOF MAV-propeller setup and its unstable response.

prone to breaking.

VI. Conclusion

The flight dynamics of flapping micro-air-vehicles (MAVs) are studied in the longitudinal plane near the hovering equilibrium. The system is a nonlinear, time-periodic with a large separation between the systems's two time scales, which invokes averaging. Using direct averaging, it is found that flapping MAVs are unstable at hover; mainly due to lack of pitch stiffness. However, using more rigorous mathematical tools (higher-order averaging based on chronological calculus), it is shown that the high-frequency oscillatory aerodynamic forces induce a vibrational stabilization mechanism resulting in a pitch stiffness. This unconventional stabilization technique is mainly due to the interaction between the fast wing flapping dynamics and the slow body dynamics, which cannot be captured by direct averaging. An experimental setup that allows for two degrees of freedom for the body (forward motion and pitching motion) is constructed to verify/demonstrate such a phenomenon. Recalling that vibrational control is an *open loop* stabilization technique due to the application of a *sufficiently high frequency periodic forcing*, the stability of the system is studied at different flapping frequencies. It is found that the system is naturally (without feedback) stabilized beyond a certain threshold of the flapping frequency (15Hz in the current setup), which conforms with the vibrational control concept. Moreover, a replica of the system is constructed in which the the wings of the flapping bird are kept stationary and the thrust is produced by a propeller instead, which revolves at a constant speed. The only difference between the two setups is that the flapping system produces a periodic thrust force resulting in a time-periodic dynamics which may enjoy vibrational stabilization. In contrast, the propeller system produces a constant thrust force and, hence, time-invariant dynamics leaving no room for vibrational stabilization. It is found that the propeller system replica is unstable at all applied voltages and becomes even more unstable at larger applied voltages (i.e., when it comes closer to the hovering position), which verifies that the observed stabilization in the flapping system at high frequencies is mainly due to periodicity of the driving force (i.e., a vibrational control). This finding is important for the development of flapping micro-air-vehicles as the designer may promote such a natural stabilization mechanism dispensing a feedback control system with its sensory-control-actuator subsystem, hence, making initialization more feasible.

VII. Acknowledgments

The first author is thankful to the support of the National Science Foundation grant CMMI-1709746. The authors are very grateful to the help of Joel Navarro during his internship at UC Irvine.

References

[1] Meerkov, S. M., "Principle of vibrational control: theory and applications," *Automatic Control, IEEE Transactions on*, Vol. 25, No. 4, 1980, pp. 755–762.

[2] Stephenson, A., "On an induced stability," *The London, Edinburgh, and Dublin Philosophical Magazine and Journal of Science*, Vol. 15, No. 86, 1908, pp. 233–236.

[3] Kapitza, P. L., "Pendulum with a vibrating suspension," *Uspekhi Fiz. Nauk*, Vol. 44, No. 1, 1951, pp. 7–20.

[4] Kapitza, P. L., "Dynamical stability of a pendulum when its point of suspension vibrates," *Collected Papers by PL Kapitza*, Vol. 2, 1965, pp. 714–725.

[5] Taha, H., Tahmasian, S., Woolsey, C. A., Nayfeh, A. H., and Hajj, M. R., "The Need for Higher-Order Averaging in the Stability Analysis of Hovering MAVs/Insects," Vol. 10, No. 1, pp. 016002, Selected in the Bioinspiration & Biomimetics Highlights of 2015.

[6] Khalil, H. K., *Noninear Systems*, Prentice-Hall, New Jersey, 2002.

[7] Baillieul, J. and Lehman, B., "Open-loop control using oscillatory inputs," *CRC Control Handbook*, 1996, pp. 967–980.

[8] Berg, J. M. and Wickramasinghe, I. M., "Vibrational control without averaging," *Automatica*, Vol. 58, 2015, pp. 72–81.

[9] Ellington, C. P., "The aerodynamics of hovering insect flight: III. Kinematics," *Philosophical Transactions Royal Society London Series B*, Vol. 305, 1984, pp. 41–78.

[10] Deng, X., Schenato, L., Wu, W. C., and Sastry, S. S., "Flapping Flight for Biomemetic Robotic Insects: Part II Flight Control Design," *IEEE Transactions on Robotics*, Vol. 22, No. 4, 2006, pp. 789–803.

[11] Rozhdestvensky, K. V. and Ryzhov, V. A., "Aerohydrodynamics of flapping-wing propulsors," *Progress in Aerospace Sciences*, Vol. 39, No. 8, 2003, pp. 585–633.

[12] Wood, R. J., "The First Takeoff of a Biologically Inspired At-Scale Robotic Insect," *IEEE Transactions on Robotics and Automation*, Vol. 24, No. 2, 2008, pp. 341–347.

[13] Norberg, R. Å., "Hovering flight of the dragonfly Aeschna juncea L., kinematics and aerodynamics," *Swimming and flying in nature*, Springer, 1975, pp. 763–781.

[14] Dudley, R. and Ellington, C. P., "MECHANICS OF FORWARD FLIGHT IN BUMBLEBEES II. QUASI-STEADY LIFT AND POWER REQUIREMENTS," *Journal of Experimental Biology*, Vol. 148, 1990, pp. 53–88.

[15] Ellington, C. P., "Unsteady aerodynamics of insect flight," Vol. 49, Soc. Exp. Biol., 1995, pp. 109–129.

[16] Willmott, A. P. and Ellington, C. P., "The mechanisms of Flight in the Hawkmoth Manduca Sexta, I: Kinematics of Hovering and Forward Flight," *Journal of Experimental Biology*, Vol. 200, No. 21, 1997.

[17] Ellington, C. P., Van Den Berg, C., Willmott, A. P., and Thomas, A. L. R., "Leading-edge vortices in insect flight," *Nature*, Vol. 384, 1996, pp. 626–630.

[18] Liu, H., Ellington, C. P., Kawachi, K., Van Den Berg, C., and Willmott, A. P., "A computational fluid dynamic study of hawkmoth hovering," *The journal of experimental biology*, Vol. 201, No. 4, 1998, pp. 461–477.

[19] Thomas, A. L. R. and Taylor, G. K., "Animal flight dynamics I. Stability in gliding flight." *Journal of Theoretical Biology*, Vol. 212, No. 1, 2001, pp. 399–424.

[20] Taylor, G. K. and Thomas, A. L. R., "Dynamic Flight Stability in the Desert Locust," *Journal of Theoretical Biology*, Vol. 206, No. 6, 2003, pp. 2803–2829.

[21] Khan, Z. A. and Agrawal, S. K., "Control of Longitudinal Flight Dynamics of a Flapping Wing Micro Air Vehicle Using Time Averaged Model and Differential Flatness Based Controller," IEEE American Control Conference, 2007, pp. 5284–5289.

[22] Sun, M. and Xiong, Y., "Dynamic flight stability of a hovering bumblebee." *Journal of Experimental Biology*, Vol. 208, No. 3, 2005, pp. 447–459.

[23] Sun, M., Wang, J., and Xiong, Y., "Dynamic Flight Stability of Hovering Insects," *Acta Mechanica Sinica*, Vol. 23, No. 3, 2007, pp. 231–246.

[24] Xiong, Y. and Sun, M., "Dynamic Flight Stability of a Bumble Bee in Forward Flight," *Acta Mechanica Sinica*, Vol. 24, No. 3, 2008, pp. 25–36.

[25] Gao, N., Aono, H., and Liu, H., "A numerical analysis of dynamic flight stability of hawkmoth hovering," *Journal of Biomechanical Science and Engineering*, Vol. 4, No. 1, 2009, pp. 105–116.

[26] Schenato, L., Campolo, D., and Sastry, S. S., "Controllability Issues in Flapping Flight for Biomemetic MAVs," Vol. 6, 42nd IEEE conference on Decision and Control, 2003, pp. 6441–6447.

[27] Doman, D. B., Oppenheimer, M. W., and Sigthorsson, D. O., "Wingbeat Shape Modulation for Flapping-Wing Micro-Air-Vehicle Control During Hover," *Journal of Guidance, Control and Dynamics*, Vol. 33, No. 3, 2010, pp. 724–739.

[28] Oppenheimer, M. W., Doman, D. B., and Sigthorsson, D. O., "Dynamics and Control of a Biomimetic Vehicle Using Biased Wingbeat Forcing Functions," *Journal Guidance, Control and Dynamics*, Vol. 34, No. 1, 2011, pp. 204–217.

[29] Faruque, I. and Humbert, J. S., "Dipteran insect flight dynamics. Part 1 Longitudinal motion about hover," *Journal of theoretical biology*, Vol. 264, No. 2, 2010, pp. 538–552.

[30] Cheng, B. and Deng, X., "Translational and Rotational Damping of Flapping Flight and Its Dynamics and Stability at Hovering," *IEEE Transactions On Robotics*, Vol. 27, No. 5, 2011, pp. 849–864.

[31] Nelson, R. C., *Flight stability and automatic control*, Vol. 2, WCB/McGraw Hill New York, 1998.

[32]Sarychev, A., “Stability Criteria for Time-periodic Systems via High-order Averaging Techniques,” *Nonlinear Control in the Year 2000*, Vol. 2 of *Lecture Notes in Control and Information Sciences*, Springer-Verlag, 2001, pp. 365–377.

[33]Vela, P. A., *Averaging and control of nonlinear systems (with application to biomimetic locomotion)*, Ph.D. thesis, California Institute of Technology, Pasadena, CA, May 2003.

[34]Agrachev, A. A. and Gamkrelidze, R. V., “The exponential representation of flows and the chronological calculus,” *Matematicheskii Sbornik*, Vol. 149, No. 4, 1978, pp. 467–532.

[35]Yagasaki, K. and Ichikawa, T., “Higher-order averaging for periodically forced weakly nonlinear systems,” *International Journal of Bifurcation and Chaos*, Vol. 9, No. 03, 1999, pp. 519–531.

[36]Hartono and Van Der Burgh, A. H. P., “Higher-order averaging: periodic solutions, linear systems and an application,” *Nonlinear Analysis: Theory, Methods & Applications*, Vol. 52, No. 7, 2003, pp. 1727–1744.

[37]Nayfeh, A. H., *Perturbation Methods*, John Wiley and Sons, Inc., 1973.

[38]Sanders, J. A., Verhulst, F., and Murdock, J. A., *Averaging methods in nonlinear dynamical systems*, Vol. 2, Springer, 2007.

[39]Bullo, F., “Averaging and vibrational control of mechanical systems,” *SIAM Journal on Control and Optimization*, Vol. 41, No. 2, 2002, pp. 542–562.

[40]Taha, H., Hajj, M. R., and Nayfeh, A. H., “On the Longitudinal Flight Dynamics of Hovering MAVs/Insects,” *Journal of Guidance Control and Dynamics*, Vol. 37, No. 3, 2014, pp. 970–978.

[41]Taha, H. E., *Mechanics of Flapping Flight: Analytical Formulations of Unsteady Aerodynamics, Kinematic Optimization, Flight Dynamics, and Control*, Ph.D. thesis, Virginia Polytechnic Institute and State University, 2013.

[42]Taylor, G. K. and Thomas, A. L. R., “Animal Flight Dynamics II. Longitudinal Stability in Flapping Flight,” *Journal of Theoretical Biology*, Vol. 214, 2002.

[43]Deng, X., Schenato, L., Wu, W. C., and Sastry, S. S., “Flapping Flight for Biomemetic Robotic Insects: Part I System Modeling,” *IEEE Transactions on Robotics*, Vol. 22, No. 4, 2006, pp. 776–788.

[44]Khan, Z. A. and Agrawal, S. K., “Force and Moment Characterization of Flapping Wings for Micro Air Vehicle Application,” IEEE American Control Conference, 2005, pp. 1515–1520.

[45]Doman, D. B., Oppenheimer, M. W., and Sigthorsson, D. O., “Dynamics and Control of a Minimally Actuated Biomimetic Vehicle, Part I- Aerodynamic Model,” No. 2009-6160, AIAA Guidance, Navigation, and Control Conference, Chicago, Illinois.

[46]Oppenheimer, M. W., Doman, D. B., and Sigthorsson, D. O., “Dynamics and Control of a Minimally Actuated Biomimetic Vehicle, Part II- Control,” No. 2009-6161, AIAA Guidance, Navigation, and Control Conference, Chicago, Illinois.

[47]Oppenheimer, M. W., Doman, D. B., and Sigthorsson, D. O., “Dynamics and Control of a Biomimetic Vehicle Using Biased Wingbeat Forcing Functions: Part I: Aerodynamic Model,” No. 2010-1023, AIAA.

[48]Doman, D. B., Oppenheimer, M. W., and Sigthorsson, D. O., “Dynamics and Control of a Biomimetic Vehicle Using Biased Wingbeat Forcing Functions: Part II: Controller,” AIAA-paper 2010-1024, Jan 2010.

[49]Taha, H., Nayfeh, A. H., and Hajj, M. R., “Aerodynamic-Dynamic Interaction and Longitudinal Stability of Hovering MAVs/Insects,” AIAA-Paper 2013-1707.

[50]Taha, H., Hajj, M. R., and Beran, P. S., “Unsteady Nonlinear Aerodynamics of Hovering MAVs/Insects,” AIAA-Paper 2013-0504.

[51]Taha, H., Hajj, M. R., and Beran, P. S., “State Space Representation of the Unsteady Aerodynamics of Flapping Flight,” *Aerospace Science and Technology*, Vol. 34, 2014, pp. 1–11.

[52]Berman, G. J. and Wang, Z. J., “Energy-minimizing kinematics in hovering insect flight,” *Journal of Fluid Mechanics*, Vol. 582, No. 1, 2007, pp. 153,168.

[53]Ellington, C. P., “The aerodynamics of hovering insect flight: II. Morphological parameters,” *Philosophical Transactions Royal Society London Series B*, Vol. 305, 1984, pp. 17–40.

[54]Orlowski, C. T. and Girard, A. R., “Modeling and Simulation of the Nonlinear Dynamics of Flapping Wing MAVs,” *AIAA Journal*, Vol. 49, No. 5, 2011, pp. 969–981.

[55]Orlowski, C. T. and Girard, A. R., “Averaging of the Nonlinear Dynamics of Flapping Wing MAV for Symmetrical Flapping,” Aerospace Sciences Meeting, 2011.

[56]Banazadeh, A. and Taymourtash, N., “Adaptive attitude and position control of an insect-like flapping wing air vehicle,” *Nonlinear Dynamics*, 2016, pp. 1–20.

[57]“Gravity 360 Degree Hall Angle Sensor,” https://www.dfrobot.com/wiki/index.php/Gravity:_Hall_Angle_Sensor_SKU:_SEN0221.

[58]“DIY Electric Dove Super Capacitor Wing Flapping Bird Toy Gift,” https://www.banggood.com/Wing-Flapping-Bird-Toy-Gift-p-1013167.

[59]“Nano QX 6x15mm Ballistic 19,600kv,” https://www.amazon.com/Apex-RC-Products-Inductrix-Ballistic/dp/B0711251VV/ref=pd_ybh_a_

[60]“Object Detection - Color Filtering - OpenCV - C++,” http://jematoscv.blogspot.com/search/label/Projects.

[61]Wu, J. H., Zhang, Y. L., and Sun, M., “Hovering of model insects: simulation by coupling equations of motion with Navier-Stokes equations,” *The Journal of Experimental Biology*, Vol. 212, No. 20, 2009, pp. 3313–3329.

[62]Su, W. and Cesnik, C. E. S., “Flight Dynamic Stability of a Flapping Wing Micro Air Vehicle in Hover,” AIAA-Paper 2011-2009.

[63]Taha, H., Nayfeh, A. H., and Hajj, M. R., “Effect of the Aerodynamic-Induced Parametric Excitation on the Longitudinal Stability of Hovering MAVs/Insects,” *Nonlinear Dynamics*, Vol. 78, No. 4, 2014, pp. 2399–2408.